

Frustrated trimer chain: Model for $\text{Cu}_3\text{Cl}_6(\text{H}_2\text{O})_2 \cdot 2\text{H}_8\text{C}_4\text{SO}_2$ in a magnetic field ?

A. Honecker¹ and A. Läuchli²

¹ Institut für Theoretische Physik, TU Braunschweig, Mendelssohnstr. 3, D-38106 Braunschweig, Germany.

² Institut für Theoretische Physik, ETH-Hönggerberg, CH-8093 Zürich, Switzerland.

(May 24, 2000)

Recent magnetization and susceptibility measurements on $\text{Cu}_3\text{Cl}_6(\text{H}_2\text{O})_2 \cdot 2\text{H}_8\text{C}_4\text{SO}_2$ by Ishii *et.al.* [J. Phys. Soc. Jpn. **69**, 340 (2000)] have demonstrated the existence of a spin gap. In order to explain the opening of a spin gap in this copper-trimer system, Ishii *et.al.* have proposed a frustrated trimer chain model. Since the exchange constants for this model have not yet been determined, we develop a twelfth-order high-temperature series for the magnetic susceptibility and fit it to the experimentally measured one. We find that some of the coupling constants are likely to be *ferromagnetic*. The combination of several arguments does not provide any evidence for a spin gap in the parameter region with ferromagnetic coupling constants, but further results e.g. for the magnetization process are in qualitative agreement with the experimental observations.

PACS numbers: 75.50.Ee, 75.40.Mg, 75.45.+j

I. INTRODUCTION

The trimerized $S = 1/2$ Heisenberg chain in a strong external magnetic field has already received a substantial amount of theoretical attention, one reason being a plateau at one third of the saturation magnetization in the magnetization curve [1–5]. Some frustrated variants of the trimer model have also been investigated [6–10] since they can be shown to have dimer groundstates and thus a spin gap.

While many materials with trimer constituents exist (see e.g. [11]), the behavior in high magnetic fields has been investigated only in a few of them, for instance in $3\text{CuCl}_2 \cdot 2\text{dioxane}$ [12]. Also $\text{Cu}_3\text{Cl}_6(\text{H}_2\text{O})_2 \cdot 2\text{H}_8\text{C}_4\text{SO}_2$ belongs to the known trimer materials [13,14], but its behavior in a strong magnetic field has been measured only recently [15] and at the same time its magnetic susceptibility has been remeasured. Surprisingly, a spin gap of about 3.9Tesla (that is roughly 5.5K) is observed both in the magnetic susceptibility of $\text{Cu}_3\text{Cl}_6(\text{H}_2\text{O})_2 \cdot 2\text{H}_8\text{C}_4\text{SO}_2$ [16] as well as in the magnetization as a function of external magnetic field. This system probably exhibits also a plateau at one third of the saturation magnetization in addition to the spin gap.

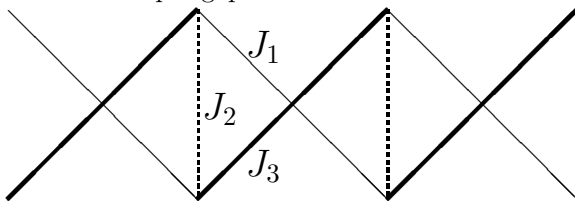


FIG. 1. The frustrated trimer chain model. All corners and intersections carry a spin $1/2$ coupled with exchange constants indicated by the connecting lines.

Motivated by the crystal structure [13], the authors of [15] have proposed the following model (see also Fig. 1) [17]:

$$\begin{aligned}
 H = & J_1 \sum_{i=1}^{L/3} \{ \mathbf{S}_{3i} \cdot \mathbf{S}_{3i+1} + \mathbf{S}_{3i+1} \cdot \mathbf{S}_{3i+2} \} \\
 & + J_2 \sum_{i=1}^{L/3} \mathbf{S}_{3i+2} \cdot \mathbf{S}_{3i+3} \\
 & + J_3 \sum_{i=1}^{L/3} \{ \mathbf{S}_{3i+1} \cdot \mathbf{S}_{3i+3} + \mathbf{S}_{3i+2} \cdot \mathbf{S}_{3i+4} \} \\
 & - h \sum_{i=1}^L S_i^z.
 \end{aligned} \tag{1.1}$$

Since the spin is localized on Cu^{2+} ions, the \mathbf{S}_i are spin- $1/2$ operators at site i . In (1.1), the reduced field h is related to the physical field H by $h = g\mu_B H$ in units where $k_B = 1$. The numerical prefactor is determined by $\mu_B \approx 0.67171\text{K/Tesla}$ as well as the value of g which for the present material is slightly above 2 (the precise numerical value depends on the direction of the external magnetic field relative to the crystal axes).

For a study of the phase diagram of the Hamiltonian (1.1), it is useful to observe that the Hamiltonian and therefore also the phase diagram are invariant under the exchange of J_1 and J_3 such that one can concentrate e.g. on $|J_3| \leq |J_1|$. In fact, the $h = 0$ phase diagram with antiferromagnetic exchange constants ($J_i \geq 0$) has been explored in [18] using bosonization and exact diagonalization (see also [19]) determining in particular a parameter region with a spin gap. Very recently, this was complemented by a computation of the magnetization curve at some values of the parameters using DMRG [20]. The investigations of [18–20] concentrated on the region with all coupling constants in (1.1) antiferromagnetic ($J_i \geq 0$) because [15] suggested that this should be appropriate for $\text{Cu}_3\text{Cl}_6(\text{H}_2\text{O})_2 \cdot 2\text{H}_8\text{C}_4\text{SO}_2$. However, the parameters

relevant to the experimental system have not really been determined so far. We believe that this is an important issue in particular in view of the fact that according to the crystallographic data [13], all angles of the Cu–Cl–Cu bonds lie in the region of 91° to 96° – a region where usually no safe inference on the coupling constants J_i can be made, not even about their signs. We will therefore develop a high-temperature series for the magnetic susceptibility of the model (1.1) and use it to *determine* the coupling constants from the experimental data [15]. It will turn out that some coupling constants are likely to be *ferromagnetic*, *i.e.* the experimentally relevant coupling constants lie presumably outside the region studied so far. We then proceed to study more general properties of the model and to address the question of a spin gap in the relevant parameter region. We use mainly perturbative arguments supplemented by numerical methods.

Some supplementary results on the trimer model which are not directly relevant to $\text{Cu}_3\text{Cl}_6(\text{H}_2\text{O})_2 \cdot 2\text{H}_8\text{C}_4\text{SO}_2$ are contained in an appendix or can be found in [21].

II. MAGNETIC SUSCEPTIBILITY AND SPECIFIC HEAT

A. High-temperature series for zero field

First we discuss some high-temperature series in zero magnetic field. We have used an elementary approach to

The lowest orders of a reduced magnetic susceptibility χ

$$\begin{aligned} \chi_{\text{red.}}(\beta) &= \frac{1}{\beta L Z_L} \frac{\partial^2}{\partial h^2} \text{tr} \left(e^{-\beta(H_0 - h S_{\text{tot}}^z)} \right) \Big|_{h=0} = \frac{\beta}{L} \frac{\text{tr} \left((S_{\text{tot}}^z)^2 e^{-\beta H_0} \right)}{Z_L} \\ &= \frac{\beta}{4} - \frac{\beta^2}{24} (2J_3 + J_2 + 2J_1) - \frac{\beta^3}{96} (J_1^2 + J_2^2 + J_3^2 - 6J_3J_1 - 2J_2J_1 - 2J_3J_2) \\ &\quad + \frac{\beta^4}{1152} (8J_3^3 - 3J_3^2J_2 + 6J_2^2J_1 + 6J_3J_2^2 + 8J_1^3 - 3J_2J_1^2 + J_2^3) \\ &\quad + \frac{\beta^5}{4608} (-28J_3^2J_2J_1 - 28J_3J_1^2J_2 + 36J_3^2J_1^2 + 8J_3^2J_2^2 + 8J_2^2J_1^2 - 2J_3^3J_1 - 34J_3J_1^3 - 34J_3^3J_1 \\ &\quad - 10J_2J_1^3 - 2J_3J_2^3 - 10J_3^3J_2 - 28J_3J_1J_2^2 + 14J_1^4 + 14J_3^4 + 5J_2^4) \\ &\quad + \mathcal{O}(\beta^6). \end{aligned} \quad (2.2)$$

Similarly, we obtain the lowest orders of the high-temperature series for the specific heat

$$\begin{aligned} \frac{c_v(\beta)}{k_B} &= \frac{\beta^2}{L} \frac{\partial^2}{\partial \beta^2} \ln(Z_L) \\ &= \frac{\beta^2}{16} (2J_1^2 + J_2^2 + 2J_3^2) + \frac{\beta^3}{32} (2J_3^3 + 2J_1^3 + J_2^3 - 6J_3J_1J_2) \\ &\quad - \frac{\beta^4}{256} (8J_3^2J_2J_1 + 8J_3J_1^2J_2 + 12J_3^2J_1^2 + 8J_3^2J_2^2 + 8J_2^2J_1^2 + 6J_1^4 + 6J_3^4 + J_2^4 + 8J_3J_1J_2^2) \\ &\quad + \mathcal{O}(\beta^5). \end{aligned} \quad (2.3)$$

Complete 12th order versions of both series can be accessed via [21].

For a uniform Heisenberg chain ($J_1 = J_2$ and $J_3 = 0$), the coefficients of the series for χ and $\ln(Z_L)/L$ (or c_v) agree with those given for instance in [23] when they overlap.

perform the computations. Denote the Hamiltonian of a length L chain with $h = 0$ by H_0 . Then the fundamental ingredient for any higher-order expansion is that contributions of $\text{tr}(H_0^N)$ to suitable physical quantities become independent of the system size L if one uses a long enough chain with periodic boundary conditions. The concrete Hamiltonian H_0 given by (1.1) must be applied $2L/3$ times to wind once around the system and to feel that it is finite. On the other hand, contributions from $\text{tr}(H_0^N)$ with $N < 2L/3$ are independent of L . We have used this observation to determine the high-temperature series by simply computing the traces for the lowest powers N on a chain with a fixed L and periodic boundary conditions [22]. Just two small refinements to this elementary approach have been made. The first one is that we computed the traces separately for all subspaces of the z -component of the total spin S_{tot}^z . This is already sufficient to obtain series for the specific heat c_v and the magnetic susceptibility χ . The second one is to make also the order $2L/3$ usable: At this order, only the coefficient of $J_1^{L/3}J_3^{L/3}$ is affected by the finiteness of the chain and this coefficient can be corrected by hand using results for a Heisenberg ring of length $2L/3$.

For notational convenience, we introduce the partition function for L sites by

$$Z_L = \text{tr} (e^{-\beta H_0}) \quad (2.1)$$

with $k_B T = 1/\beta$.

are found to be

B. Fit to the experimental susceptibility

Now we use our 12th order series for the susceptibility (2.2) to fit the experimental data [15] and thus extract values for the coupling constants J_i . We used the data for the single crystal ($H \parallel b$ -axis) and the polycrystalline sample [15] as well as some unpublished new measurements for all three axes of a single crystal [24]. For the polycrystalline case the average g -factor is known to be $g_{av} \approx 2.1$ from ESR while in the single crystal case [15] we used the g -factor as a fitting parameter. The following prefactors are used to match the series (2.2) to the experimental data:

$$\chi_{\text{exp.}}(T) = \frac{3N_A g^2 \mu_B^2}{k_B} \chi_{\text{red.}}\left(\frac{1}{T}\right). \quad (2.4)$$

We performed fits in various intervals of temperature with a lower boundary (T_l) lying between 150K and 250K, while the upper boundary was kept fixed at 300K. Fits were performed with the raw 12th order series. For both experimental data sets of [15] we obtained reasonable, though volatile fits around $T_l = 150K - 250K$ yielding the following estimates: $J_1 = -250K \pm 40K$, $J_2 = 250K \pm 40K$, $J_3 = -40K \pm 30K$. For the single crystal sample we additionally determined $g_b = 1.95 \pm 0.05$.

We have further performed fits to unpublished single-crystal data sets where the g -factors are known from ESR [24]. When a constant is added to (2.2), the data for all three crystal axes can be fitted consistently with $J_1 \approx -300K$, $J_2 \approx 280K$ and $J_3 \approx -60K$ in an interval of high temperatures ($220K \lesssim T \leq 300K$). This set of coupling constants is in agreement with our earlier fits and we will use the latter in the further discussion below.

Fig. 2 shows the measured susceptibility for the polycrystalline sample [15] together with the series result. Since the parameters were obtained from a fit which was performed with a different data set, we have used $g = 2.03$ (which differs slightly from the experimentally found $g_{av} \approx 2.1$) in order to obtain agreement of the raw series with the experimental data for $T \geq 240K$. Clearly, the raw series should not be trusted down into the region of the maximum of χ where Padé approximants should be used instead. The region below the maximum cannot be expected to be described with a high-temperature series. The overall agreement is reasonable though the theoretical result does not reproduce the experimental one accurately in the vicinity of the maximum. This discrepancy might be due to the frustration in the model which could lead to cancellations in the coefficients. The agreement for intermediate temperatures can be improved if the maximum is included in the fitting region and Padé approximants are used in the fit. The main change with respect to the fits discussed above is that J_3 tends to be closer to J_1 . However, it will become clear from the discussion in later sections that the region with J_3 close to J_1 is not appropriate to describe the experimental observations of the low-temperature region.

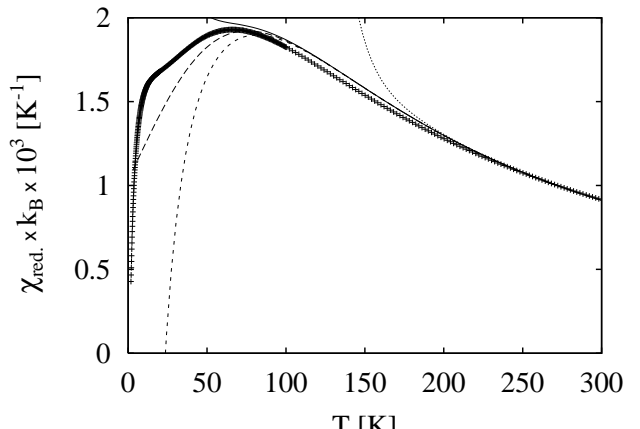


FIG. 2. Experimental results for the susceptibility ('+') in comparison with the fit $J_1 = -300K$, $J_2 = 280K$ and $J_3 = -60K$. We show the raw 12th order series (dotted line) as well as several Padé approximants: [7,6] (full line), [6,6] (long dashes) and [6,5] (short dashes).

Although we are not able to determine the coupling constants to high accuracy, all our fits lead to the conclusion that J_2 should be antiferromagnetic and J_1 and J_3 (or at least one of them) must be *ferromagnetic* if one wants to model the susceptibility measured at high temperatures [15] with the frustrated trimer chain (1.1). In view of earlier theoretical investigations [18–20], this conclusion is somewhat surprising. It further necessitates a detailed re-analysis of the Hamiltonian (1.1) since these earlier works did not look at the appropriate parameter region.

III. LANCZOS RESULTS

In order to study the zero-temperature behavior of the frustrated trimer chain we have performed Lanczos diagonalizations of small clusters with periodic boundary conditions. Although computations were performed for various values of the parameters, we will present results only for the final parameter set determined above. Further results in the region $J_i > 0$ are in agreement with [18–20].

Fig. 3 presents the zero-temperature magnetization curve for the trimer chain model. Here and below the magnetization $\langle M \rangle$ is normalized to saturation values ± 1 . First, it is reassuring that the system still has antiferromagnetic features despite two ferromagnetic coupling constants (note that we are now probing a region far from that used for determining the J_i). Since experiments found a spin gap [15], an important question clearly is if we also obtain a gap from the model with these parameters. We have therefore performed a finite-size analysis of the gap to $S^z = 1$ excitations (corresponding to the first step in the finite-size magnetization curves of Fig. 3). All our approaches led to results compatible with a vanishing gap. However, it is difficult to reliably exclude a gap of a few K with system sizes $L \leq 30$. We will therefore

return to this issue later and assume for the extrapolated thick line in Fig. 3 a vanishing spin gap. In general, this extrapolation was obtained by connecting the mid-points of the steps of the $L = 30$ magnetization curve, except for $\langle M \rangle = 1$ and $\langle M \rangle = 1/3$ where the corners were used.

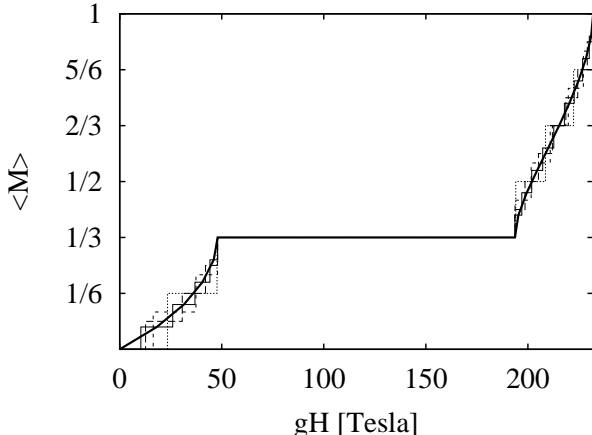


FIG. 3. Magnetization curve for $J_1 = -300\text{K}$, $J_2 = 280\text{K}$ and $J_3 = -60\text{K}$. The thick line is an extrapolation whereas thin lines are for finite system sizes: $L = 12$ (dotted), $L = 18$ (short dashes), $L = 24$ (long dashes) and $L = 30$ (full).

For the parameters of Fig. 3, $\langle M \rangle = 1/3$ is reached with a magnetic field $H = 20 - 25\text{Tesla}$. The order of magnitude agrees with the experimental finding [15] even if the value found within the model is a factor of two to three below the experimental one. Above this field, Fig. 3 exhibits a clear $\langle M \rangle = 1/3$ plateau which is expected on general grounds [1–5].

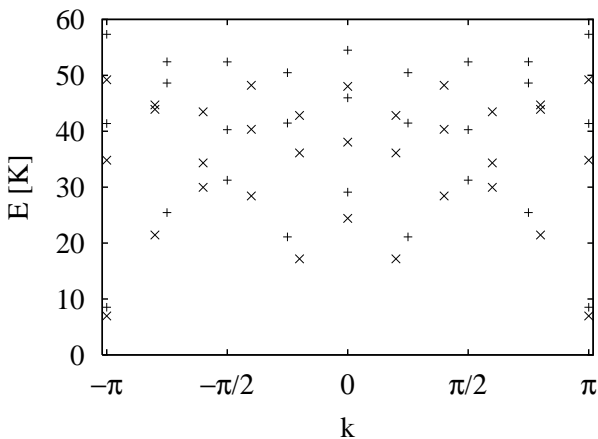


FIG. 4. Lowest three excitations in the $S^z = 1$ sector for $L = 24$ ('+') and $L = 30$ ('x') with $J_1 = -300\text{K}$, $J_2 = 280\text{K}$ and $J_3 = -60\text{K}$.

We conclude this section by presenting in Fig. 4 the lowest three excitations for the $S^z = 1$ sector as a function of momentum k , where k is measured with respect to the groundstate, *i.e.* $k = k_{S^z=1} - k_{\text{GS}}$. This spectrum is very similar to that of an $S = 1/2$ Heisenberg chain of length $L/3$ with coupling constant $J_{\text{eff.}} \approx 16\text{K}$. In particular, one can recognize the two-spinon scattering continuum and a few higher excitations. This identification of the low-energy excitations of the frustrated trimer chain

with an effective $S = 1/2$ Heisenberg chain is one of the numerical indications for the absence of a spin gap.

IV. THE LINE $J_1 = J_3$

The Lanczos results of the previous section raise the question if the trimer chain model has a spin gap in the region with $J_1, J_3 < 0$. Therefore, we proceed with further arguments to decide this issue. Since evidence for a spin gap in the parameter region $J_1, J_3 > 0$ was actually first obtained on the line $J_1 = J_3$ [10], it is interesting to see what happens for $J_1 = J_3 < 0$. The line $J_1 = J_3$ can be treated analytically at least to some extent because then the total spin is locally conserved on each bond coupled by J_2 . In fact, one can easily discuss the entire magnetization process [25] and not just the question of a spin gap. Here we will concentrate on the region $|\langle M \rangle| \leq 1/3$ because $|\langle M \rangle| > 1/3$ would require auxiliary numerical data which is not readily available. In addition, the region $|\langle M \rangle| > 1/3$ is not accessible experimentally in the trimer system $\text{Cu}_3\text{Cl}_6(\text{H}_2\text{O})_2 \cdot 2\text{H}_8\text{C}_4\text{SO}_2$ [15].

First we discuss the case $J_1 = J_3 > 0$ (we will assume $J_2 > 0$ throughout this section). In this case, the model (1.1) with $h = 0$ gives rise to three types of groundstates in different parameter regions [10]:

1. The groundstate is that of the $S = 1/2$ - $S = 1$ ferrimagnetic chain (*i.e.* $S = 1$ states on each bond coupled by J_2) for

$$J_2 < -\left(\frac{1}{2} + \epsilon_0\right) \quad (4.1)$$

with ϵ_0 the groundstate energy per site of the $S = 1/2$ - $S = 1$ ferrimagnetic chain. When we substitute the DMRG estimate [26]

$$\epsilon_0 = -0.72704 \quad (4.2)$$

into (4.1), we obtain $J_2 < 0.90816J_1$. This is consistent with the estimate $J_{2,c} = 0.909J_1$ [10] though presumably more accurate.

2. For

$$-\left(\frac{1}{2} + \epsilon_0\right) < J_2 < 2J_1 \quad (4.3)$$

the groundstate is spontaneously dimerized and thus gapful: On the bonds coupled by J_2 , singlets and triplets alternate such that the triplets couple to a spin-singlet with the two adjacent spins.

3. Finally, singlets are formed on *all* bonds coupled by J_2 for

$$J_2 > 2J_1. \quad (4.4)$$

In the first region, the system clearly behaves like a ferrimagnet with a spontaneous magnetization $\langle M \rangle = 1/3$. Also in the third case, one finds ferrimagnetic behavior with a spontaneous magnetization $\langle M \rangle = 1/3$ which arises because one third of the spins is effectively decoupled from the rest of the system and are thus polarized by an arbitrarily small magnetic field.

Only in the gapful (second) region do we find non-trivial behavior under an applied magnetic field for $|\langle M \rangle| \leq 1/3$: The magnetization jumps from $\langle M \rangle = 0$ to $\langle M \rangle = 1/3$ at

$$h = \begin{cases} J_2 + (2 + 4\epsilon_0) J_1 & \text{for } J_2 \leq J_C, \\ -J_2 + 2J_1 & \text{for } J_2 \geq J_C \end{cases} \quad (4.5)$$

with

$$J_C = -2\epsilon_0 J_1 \approx 1.45408 J_1. \quad (4.6)$$

The critical coupling J_C also separates two different $\langle M \rangle = 1/3$ plateau states: For $J_2 < J_C$ it is the $\langle M \rangle = 1/3$ state of the $S = 1/2$ - $S = 1$ ferrimagnetic chain while for $J_2 > J_C$ it consists of singlets on the J_2 -bonds alternating with polarized $S = 1/2$ spins in between. The transition between these two states at $J_2 = J_C$ can be regarded as a first-order transition.

Now we turn to the case $J_1 = J_3 < 0$ which should be more relevant to $\text{Cu}_3\text{Cl}_6(\text{H}_2\text{O})_2 \cdot 2\text{H}_8\text{C}_4\text{SO}_2$. Here the behavior turns out to be even simpler:

1. For

$$J_2 > -J_1 \quad (4.7)$$

the behavior is identical to that found in the third case above, *i.e.* the groundstate is formed by singlets on the J_2 -bonds and free $S = 1/2$ spins in between. This again gives rise to ferrimagnetic behavior with a spontaneous magnetization $\langle M \rangle = 1/3$.

2. When

$$J_2 < -J_1 \quad (4.8)$$

the entire system behaves like a ferromagnet. In this case the system is spontaneously completely polarized ($\langle M \rangle = 1$).

We conclude that –unlike for $J_1 = J_3 > 0$ – the groundstate is always gapless for $J_1 = J_3 < 0$.

V. EFFECTIVE HAMILTONIANS FOR THE GROUNDSTATE

The low-energy behavior of the model Hamiltonian (1.1) can be analyzed further using degenerate perturbation theory. Truncation at a certain order of the coupling constants leads to effective Hamiltonians which in some cases turn out to be well-known models.

We will use the abbreviations

$$\tilde{J}_i = \frac{J_i}{J_1}, \quad \bar{J}_i = \frac{J_i}{J_2}. \quad (5.1)$$

A. J_1 large and antiferromagnetic

To test the method, we first consider the case of antiferromagnetic J_1 . For this purpose we extend the first-order effective Hamiltonian of [20] for the case $J_1 \gg J_2, J_3 \geq 0$ to second order. For J_1 large and antiferromagnetic, the groundstate-space of a trimer is given by an $S = 1/2$ representation. In this subspace of doublets, the effective Hamiltonian has the form of a J_1 - J_2 chain when truncated after the second order:

$$H_{\text{eff.}} = \mathcal{J}_1 \sum_i \mathbf{S}_i \cdot \mathbf{S}_{i+1} + \mathcal{J}_2 \sum_i \mathbf{S}_i \cdot \mathbf{S}_{i+2}. \quad (5.2)$$

Here, the \mathbf{S}_i are effective spin-1/2 operators. The effective exchange constants are

$$\frac{\mathcal{J}_1}{J_1} = \frac{4}{9} \left(-\tilde{J}_3 + \tilde{J}_2 \right) - \frac{79}{405} \tilde{J}_3^2 + \frac{8}{135} \tilde{J}_2 \tilde{J}_3 + \frac{211}{1620} \tilde{J}_2^2 \quad (5.3)$$

and

$$\frac{\mathcal{J}_2}{J_1} = -\frac{91}{486} \tilde{J}_3^2 + \frac{22}{243} \tilde{J}_2 \tilde{J}_3 + \frac{10}{243} \tilde{J}_2^2. \quad (5.4)$$

In this approximation, the ferrimagnetic phase found in [18] is given by an effective ferromagnetic Hamiltonian ($\mathcal{J}_1 < 0$) while the antiferromagnetic phase corresponds to $\mathcal{J}_1 > 0$. The transition line can thus be determined from $\mathcal{J}_1 = 0$ [27]. We find

$$\begin{aligned} \tilde{J}_3 &= \frac{12}{79} \tilde{J}_2 - \frac{90}{79} + \frac{1}{158} \sqrt{17245 \tilde{J}_2^2 + 48240 \tilde{J}_2 + 32400} \\ &= \tilde{J}_2 - \frac{1}{80} \tilde{J}_2^2 + \mathcal{O}(\tilde{J}_2^3), \end{aligned} \quad (5.5)$$

which improves the agreement of the approximation $\tilde{J}_3 = \tilde{J}_2$ [20] with the numerical results of [18].

The dimer phase with a spin gap is characterized by $\mathcal{J}_2/\mathcal{J}_1 > 0.241167(5)$ (see [28] and references therein). Using (5.3) and (5.4), it is found to open at $\tilde{J}_2 \approx 3.60$, $\tilde{J}_3 \approx 1.361$ with a square-root like behavior of \tilde{J}_3 as a function of \tilde{J}_2 . Since this is not in the weak-coupling region, it is not surprising that the numbers differ substantially from those obtained numerically in [18]. However, the topology of the groundstate phase diagram comes out correctly from our effective Hamiltonian: In particular, the dimerized spin gap phase is located inside the antiferromagnetic phase and arises because of a sufficiently large effective second neighbor frustration \mathcal{J}_2 .

B. J_2 large and antiferromagnetic

The preceding argumentation is not applicable to the region $J_2 > 0$, $J_1, J_3 < 0$. However, a similar case has been discussed earlier [1,4] and $J_2 \gg |J_1|, |J_3|$ has been found to be a useful limiting case. We will now analyse this region in the same manner as above.

For $J_2 \gg |J_1|, |J_3|$, the spins on all J_2 -bonds couple to singlets and only the intermediate spins contribute to the low-energy excitations. In the space of these intermediate spins, we can again map the Hamiltonian (1.1) to the Hamiltonian (5.2) to the lowest orders in J_1, J_3 . Up to fifth order, we find the effective coupling constants to be given by [29]

$$\frac{\mathcal{J}_1}{J_2} = (\bar{J}_1 - \bar{J}_3)^2 \left\{ \frac{1}{2} + \frac{3(\bar{J}_1 + \bar{J}_3)}{4} + 3\bar{J}_1\bar{J}_3 - \frac{(\bar{J}_1 + \bar{J}_3)(107(\bar{J}_1^2 + \bar{J}_3^2) - 406\bar{J}_1\bar{J}_3)}{64} \right\} \quad (5.6)$$

and

$$\frac{\mathcal{J}_2}{J_2} = \frac{(\bar{J}_1 + \bar{J}_3)(\bar{J}_1 - \bar{J}_3)^4}{4}. \quad (5.7)$$

This mapping is now applicable regardless of the sign of J_1 and J_3 as long as $J_2 > 0$. First we consider the case of antiferromagnetic $J_1, J_3 > 0$. Then the effective coupling constants are essentially always antiferromagnetic, *i.e.* $\mathcal{J}_1, \mathcal{J}_2 > 0$ leading to a frustrated chain. If J_1 and J_3 are large enough, $\mathcal{J}_2/\mathcal{J}_1$ can exceed the critical value of about 0.241 (see above) and a spin gap opens. These observations are again in qualitative agreement with the phase diagram of [18]. As for the preceding limit, one should not expect good quantitative agreement since the required values of J_1 and J_3 are not small but of the same order as J_2 .

Now we turn to the more interesting case $J_1, J_3 < 0$. Then the oupling constant (5.7) is always ferromagnetic:

$\mathcal{J}_2 < 0$. If $|J_1|$ and $|J_3|$ are large enough, \mathcal{J}_1 also becomes ferromagnetic. This is compatible with the behavior found in section IV on the line $J_1 = J_3 < 0$. If $|J_1|$ and $|J_3|$ are small, \mathcal{J}_1 remains antiferromagnetic. Since \mathcal{J}_2 is always ferromagnetic, no frustration arises and a spin gap is *not* expected to open. This is true to the order which we have considered. Higher orders might actually yield frustrating contributions. In any case, frustration is substantially weaker for ferromagnetic $J_1, J_3 < 0$ than for antiferromagnetic $J_1, J_3 > 0$. It is therefore plausible that a spin gap is absent in the ferromagnetic region (unless $|J_1|$ and/or $|J_3|$ are very large and the present argument is not applicable).

It should be noted that (5.6) and (5.7) turn out to be small if $\bar{J}_1 - \bar{J}_3$ is small. In fact, one can argue that the results of this section remain qualitatively correct for $\bar{J}_1 - \bar{J}_3$ small even if \bar{J}_1 and \bar{J}_3 are not separately small: For $J_1 = J_3$, the intermediate spins are effectively decoupled due to the presence of the singlets on the J_2 -bonds (see section IV). A small detuning $J_1 \neq J_3$ generates an effective coupling of the intermediate spins via higher-order processes. However, the effective coupling will stay small as long as $J_1 - J_3$ is small. If one wants to model $\text{Cu}_3\text{Cl}_6(\text{H}_2\text{O})_2 \cdot 2\text{H}_8\text{C}_4\text{SO}_2$, $|J_1 - J_3|$ must therefore at least be on the same scale as e.g. the field $h \approx 80\text{K}$ required to polarize the intermediate spins leading to $\langle M \rangle = 1/3$ [15]. This observation rules out a J_1 very close to J_3 .

C. J_1 large and ferromagnetic

Finally, we calculated the effective Hamiltonian for a strong ferromagnetic intra-trimer interaction J_1 . The noninteracting groundstates are then built from products of trimer $S = 3/2$ states. Up to second order we find the following effective Hamiltonian in this subspace of low-lying trimer quartets:

$$H_{\text{eff.}} = \mathcal{J}_a \sum_i \mathbf{S}_i \cdot \mathbf{S}_{i+1} + \mathcal{J}_b \sum_i \mathbf{S}_i \cdot \mathbf{S}_{i+2} + \mathcal{J}_c \sum_i (\mathbf{S}_i \cdot \mathbf{S}_{i+1})^2 + \frac{\mathcal{J}_d}{2} \sum_i \{(\mathbf{S}_i \cdot \mathbf{S}_{i+1})(\mathbf{S}_{i+1} \cdot \mathbf{S}_{i+2}) + (\mathbf{S}_{i+2} \cdot \mathbf{S}_{i+1})(\mathbf{S}_{i+1} \cdot \mathbf{S}_i)\}, \quad (5.8)$$

where the \mathbf{S}_i are now effective spin-3/2 operators.

The coupling constants are found to be:

$$\begin{aligned} \mathcal{J}_a &= \frac{1}{9}(J_2 + 2J_3) + \frac{197J_2^2 + 212J_2J_3 + 212J_3^2}{2592|J_1|}, \\ \mathcal{J}_b &= \frac{2J_2^2 + 5J_2J_3 + 2J_3^2}{27|J_1|}, \\ \mathcal{J}_c &= \frac{41J_2^2 + 100J_2J_3 + 36J_3^2}{1296|J_1|}, \end{aligned}$$

$$\mathcal{J}_d = -\frac{4(2J_2^2 + 5J_2J_3 + 2J_3^2)}{243|J_1|}. \quad (5.9)$$

Even if this effective Hamiltonian is not a well-known one, it is clear that there is no spin gap in first order, since then the system is effectively a nearest neighbor $S = 3/2$ Heisenberg chain which is either gapless ($J_2 + 2J_3 > 0$) or ferromagnetic ($J_2 + 2J_3 < 0$).

If one neglects the \mathcal{J}_c and \mathcal{J}_d terms, one obtains a frustrated $S = 3/2$ chain which has been investigated with

DMRG and leads to a gap for $\mathcal{J}_b/\mathcal{J}_a \gtrsim 0.3$ [30]. It seems to be possible to obtain antiferromagnetic \mathcal{J}_a and \mathcal{J}_b in this region if J_2 and J_3 are chosen suitably and large (a region including the coupling constants determined in section II B). However, then one is not in the perturbative region anymore and the \mathcal{J}_c and \mathcal{J}_d terms may also become important. Further discussion is therefore needed for reliable conclusions about a gap on the basis of the Hamiltonian (5.8) with coupling constants (5.9). We simply list them here to open the way for further investigation.

VI. MAGNETIZATION PLATEAUX

Finally we digress a bit from experimentally relevant issues and discuss plateaux in the magnetization curves of the frustrated trimer chain model.

A. Magnetization one third

First we briefly comment on the region $J_1 > 0$. The trimer model has a clear plateau with $\langle M \rangle = 1/3$ if

Now we turn to the limit of large J_2 which also permits to analyze ferromagnetic J_1 (and J_3). The 11th order series of [4] for the boundaries of the $\langle M \rangle = 1/3$ plateau are readily generalized to accomodate the additional coupling constant. The boundaries are characterized by excitations with $k = \pi$. This leads to series for the lower and upper critical fields whose lowest six orders read

$$\frac{h_{c1}^{(\pi)}}{J_2 (\bar{J}_1 - \bar{J}_3)^2} = 1 + \frac{3(\bar{J}_1 + \bar{J}_3)}{2} + 6\bar{J}_1\bar{J}_3 - \frac{(\bar{J}_1 + \bar{J}_3)(107(\bar{J}_1^2 + \bar{J}_3^2) - 406\bar{J}_1\bar{J}_3)}{32} - \frac{(1185(\bar{J}_1^4 + \bar{J}_3^4) + 2104(\bar{J}_1^3\bar{J}_3 + \bar{J}_1\bar{J}_3^3) - 12722\bar{J}_1^2\bar{J}_3^2)}{256}, \quad (6.1)$$

$$\frac{h_{c2}^{(\pi)}}{J_2 (\bar{J}_1 - \bar{J}_3)^2} = \frac{1}{(\bar{J}_1 - \bar{J}_3)^2} + \frac{\bar{J}_1 + \bar{J}_3}{2(\bar{J}_1 - \bar{J}_3)^2} - \frac{(\bar{J}_1 + \bar{J}_3)}{4} - \frac{(5(\bar{J}_1^2 + \bar{J}_3^2) + 30\bar{J}_1\bar{J}_3)}{64} + \frac{(\bar{J}_1 + \bar{J}_3)(19(\bar{J}_1^2 + \bar{J}_3^2) - 102\bar{J}_1\bar{J}_3)}{128} + \frac{(11(\bar{J}_1^4 + \bar{J}_3^4) - 6(\bar{J}_1^3\bar{J}_3 + \bar{J}_1\bar{J}_3^3) - 874\bar{J}_1^2\bar{J}_3^2)}{512}, \quad (6.2)$$

respectively.

Complete 11th order versions of both series can again be accessed through [21]. The series eq. (14) of [4] are recovered from (6.1) and (6.2) when one substitutes either $J_1 = 0$ or $J_3 = 0$. It should be noted that already in [4] poor convergence of h_{c1} was observed in the region of interest, *i.e.* where some $|\bar{J}_i|$ becomes of order unity.

The main conclusion of this section is that a clear plateau with $\langle M \rangle = 1/3$ is expected at least in the regions where one of the coupling constants is large.

B. Possibility of a plateau at $\langle M \rangle = 2/3$

When a spin gap opens in the frustrated trimer model, the groundstate is dimerized, *i.e.* translational invariance

$|J_2|, |J_3| \ll J_1$ [4]. Series for its boundaries can be obtained by generalizing the computation of [4] if we assume first that the boundaries are determined by single-spin flips and secondly make some assumptions on the momenta k of the relevant excitations.

We have computed these series for generic k up to fourth order and for special values of k up to fifth order. We do not present them here; they can be accessed via [21]. We leave a detailed analysis to the interested reader and just make a few comments. The series imply a clear $\langle M \rangle = 1/3$ plateau in the entire weak-coupling region which can be further substantiated numerically. The dispersion of the excitation at the lower boundary of this plateau indicates the existence of an incommensurate region which is very similar to that found for the frustrated J_1 - J_2 chain in a magnetic field (see [31] and references therein). In fact, the existence of such an incommensurate region is expected already from the mappings of the frustrated trimer chain to the frustrated J_1 - J_2 chain which we discussed in section V.

is spontaneously broken by a period two. Spontaneous breaking of translational invariance by a period two also permits the appearance of a plateau with $\langle M \rangle = 2/3$ (see [31] and references therein). We will now investigate this possibility further.

First we consider again the case $J_1 > 0$ and start in the limit of strong trimerization ($J_2 = 0, J_3 = 0$). When one applies a magnetic field $h_c = \frac{3}{2}J_1$, the two states $|\uparrow\uparrow\uparrow\rangle$ and $\frac{1}{\sqrt{6}}(|\downarrow\uparrow\uparrow\rangle - 2|\uparrow\downarrow\uparrow\rangle + |\uparrow\uparrow\downarrow\rangle)$ are degenerate in energy. This degeneracy is then lifted by the couplings J_2, J_3 . The effective Hamiltonian to first order is an XXZ chain in a magnetic field [32–37,31]. We obtain the following effective couplings for the XXZ chain:

$$J_{xy} = \frac{1}{6}J_2 - \frac{2}{3}J_3$$

$$J_z = \frac{1}{36}(J_2 + 8J_3)$$

$$h_{\text{eff}} = h - h_c - \frac{1}{36}(5J_2 + 22J_3) \quad (6.3)$$

and therefore the effective anisotropy $\Delta_{\text{eff}} = J_z/|J_{xy}|$ is

$$\Delta_{\text{eff}} = \frac{J_2 + 8J_3}{|6J_2 - 24J_3|}. \quad (6.4)$$

For $5/32 < J_3/J_2 < 7/16$, we have $\Delta_{\text{eff}} > 1$ and thus a gap, *i.e.* an $\langle M \rangle = 2/3$ plateau in the original model. A plateau with $\langle M \rangle = 2/3$ can be indeed observed numerically somewhere in this region (see e.g. [20]). The line $J_3/J_2 = 1/4$ describes the Ising limit $\Delta_{\text{eff}} = \infty$.

In order to address the region of ferromagnetic J_1 , we now start from the limit $J_1 = J_3 = 0$ and apply a magnetic field $h_c = J_2$. Then the two states $|\uparrow\uparrow\rangle$ and $\frac{1}{\sqrt{2}}(|\downarrow\uparrow\rangle - |\uparrow\downarrow\rangle)$ on the J_2 -dimer become degenerate in energy while the intermediate spins are already polarized. This can be again treated by degenerate perturbation theory in $1/J_2$. Up to third order we find an XXZ chain with

$$\frac{J_{xy}}{J_2} = \frac{1}{8}(2 + \bar{J}_1 + \bar{J}_3)(\bar{J}_1 - \bar{J}_3)^2$$

$$\frac{J_z}{J_2} = \frac{1}{8}(\bar{J}_1 + \bar{J}_3)(\bar{J}_1 - \bar{J}_3)^2$$

$$\frac{h_{\text{eff}}}{J_2} = \frac{h}{J_2} - 1 - \frac{1}{2}(\bar{J}_1 + \bar{J}_3) - \frac{1}{4}(\bar{J}_1 - \bar{J}_3)^2 \quad (6.5)$$

that is

$$\Delta_{\text{eff}} = \frac{\bar{J}_1 + \bar{J}_3}{|2 + \bar{J}_1 + \bar{J}_3|}. \quad (6.6)$$

In the region where this treatment is valid, we always have a small Δ_{eff} , *i.e.* no plateau at $\langle M \rangle = 2/3$. Indeed, one can see that the dimer excitations can hop at second order in $1/J_2$ while up to this order all diagonal terms involve only a single dimer site. Thus, up to second order the diagonal terms contribute only to h_{eff} and to this order one obtains an XY chain in a magnetic field. A small anisotropy is restored at third order before terms that are not described by a simple XXZ chain arise at fourth order.

VII. CONCLUSIONS

We have studied the frustrated trimer chain (1.1) (Fig. 1) using a variety of methods. First, we have computed 12th-order high-temperature series for the susceptibility χ and specific heat. Fits of the high-temperature tail of the susceptibility computed from the model to the one measured on $\text{Cu}_3\text{Cl}_6(\text{H}_2\text{O})_2 \cdot 2\text{H}_8\text{C}_4\text{SO}_2$ [15] lead to $J_2 = 250\text{K} \pm 40\text{K}$ and unexpectedly [15,18–20] to *ferromagnetic* $J_1 = -260\text{K} \pm 50\text{K}$, $J_3 = -40\text{K} \pm 30\text{K}$. We assumed that these parameters remain valid down

to low temperatures since we are not aware of any indication of a drastic change in the magnetic behavior of $\text{Cu}_3\text{Cl}_6(\text{H}_2\text{O})_2 \cdot 2\text{H}_8\text{C}_4\text{SO}_2$ as temperature is lowered. In fact, features of other experimental observations at intermediate and low temperatures are roughly reproduced with the aforementioned parameters: We find a maximum in $\chi(T)$ in the region $50\text{K} \leq T \leq 100\text{K}$ and a smooth increase of the low-temperature magnetization $\langle M \rangle$ from 0 to $1/3$ as the external magnetic field is increased from zero to several ten Tesla. From a quantitative point of view, the agreement may however not yet be entirely satisfactory: Deviations between the measured susceptibility from the one obtained within the model can be seen in the interval $80\text{K} \leq T \leq 200\text{K}$ and the model predicts an $\langle M \rangle = 1/3$ magnetization for a magnetic field that is a factor two to three below the one actually required in the experiment.

Probably the most exciting experimental observation [15] for $\text{Cu}_3\text{Cl}_6(\text{H}_2\text{O})_2 \cdot 2\text{H}_8\text{C}_4\text{SO}_2$ is the existence of a spin gap of about 5.5K . We have therefore searched for a spin gap in the region of ferromagnetic J_1 and J_3 using several methods. Neither Lanczos diagonalization, discussion of the line $J_1 = J_3$ nor an effective Hamiltonian for large J_2 provide any evidence in favor of a spin gap in this parameter region. A further careful analysis of this issue would certainly be desireable in particular in view of the small size of the actually observed gap. At present, however, it seems likely that the model does not reproduce a spin gap in the relevant parameter region.

It should be noted that the coupling constants which we have determined are about two orders of magnitude larger than the experimentally observed gap. Therefore, a small modification of the model should already be sufficient to produce a gap of this magnitude. The possibilities include dimerization of the coupling constants, exchange anisotropy as well as additional couplings. A modification of the model along these lines may also help to improve the quantitative agreement with the features observed in $\text{Cu}_3\text{Cl}_6(\text{H}_2\text{O})_2 \cdot 2\text{H}_8\text{C}_4\text{SO}_2$ at energy scales of about 100K . Further measurements are however needed to discriminate between these possibilities. For example, it would be interesting to measure the specific heat and compare it with our series (2.3). Inelastic neutron scattering would presumably be most helpful: First, this should clearly decide if $\text{Cu}_3\text{Cl}_6(\text{H}_2\text{O})_2 \cdot 2\text{H}_8\text{C}_4\text{SO}_2$ is really quasi-one-dimensional and secondly it would yield direct information on the excitation spectrum which could hopefully be interpreted in terms of coupling constants. Such a determination of the coupling constant would also circumvent the question whether model parameters change as a function of temperature since neutron scattering is carried out at low temperatures, *i.e.* the temperature scale of interest. We therefore hope that neutron scattering can indeed be performed and are curious if excitations will be observed that are similar to those computed in the trimer chain model (Fig. 4).

The frustrated trimer chain model is also interesting in its own right: It has a rich phase diagram which among

others includes many aspects of the J_1 - J_2 chain such as a frustration-induced spin gap in some parameter region [18–20] and incommensurate groundstates in a magnetic field. Also plateaux in the magnetization curve exist in this model: A plateau with $\langle M \rangle = 1/3$ is abundant both in the regions with antiferromagnetic and ferrimagnetic $h = 0$ groundstates. Also a plateau with $\langle M \rangle = 2/3$ can be shown to exist in the region with $J_1, J_3 > 0$ (see [20] and section VI B). Like in the case of the spin gap, the opening of the latter plateau is accompanied by spontaneous breaking of translational invariance in the groundstate. Amusingly, however, the $\langle M \rangle = 2/3$ plateau opens already for $J_2, J_3 \ll J_1$ – a region where the spin gap is absent. In this context of magnetization plateaux, we hope that the magnetization measurements [15] can be extended to slightly higher fields which should unveil the lower edge of the $\langle M \rangle = 1/3$ plateau.

ACKNOWLEDGMENTS

We are very grateful to M. Ishii and H. Tanaka for providing us with their partially unpublished data for the susceptibility and for discussions. In addition, useful discussions with D.C. Cabra, F. Mila, M. Troyer and T.M. Rice are gratefully acknowledged. A.H. is indebted to the Alexander von Humboldt-foundation for financial support during the initial stages of this work as well as to the ITP-ETHZ for hospitality.

APPENDIX: THE SATURATION FIELD

Among the simplest computations that can be performed for the model (1.1) in the presence of a magnetic field is the determination of the saturation field h_{uc} where the transition to a fully polarized state takes place.

Following [1,4], one has to determine the maximal eigenvalue of the matrix

$$\frac{1}{2} \begin{pmatrix} J_1 + J_2 + J_3 & -J_1 - J_3 e^{ik} & -J_2 e^{ik} \\ -J_1 - J_3 e^{-ik} & 2J_1 + 2J_3 & -J_1 - J_3 e^{ik} \\ -J_2 e^{-ik} & -J_1 - J_3 e^{-ik} & J_1 + J_2 + J_3 \end{pmatrix} \quad (\text{A1})$$

if this transition proceeds via a single spin-flip. It turns out that in the present case the largest eigenvalue is always located either at $k = \pi$ or $k = 0$. For $k = \pi$ we find

$$h_{\text{uc}}^{(\pi)} = \frac{1}{4} \sqrt{9(J_1^2 + J_3^2) - 4(J_1 + J_3)J_2 - 14J_1J_3 + 4J_2^2} + \frac{3}{4}(J_1 + J_3) + \frac{1}{2}J_2, \quad (\text{A2})$$

while for $k = 0$ we obtain

$$h_{\text{uc}}^{(0)} = \begin{cases} \frac{1}{2}(J_1 + J_3) + J_2 & \text{for } J_2 \geq J_1 + J_3, \\ \frac{3}{2}(J_1 + J_3) & \text{for } J_2 \leq J_1 + J_3. \end{cases} \quad (\text{A3})$$

In general, (A2) applies for $J_3 \leq (J_1J_2)/(4J_1 - J_2)$ and otherwise (A3). As a consequence, (A2) should always be used for $J_2 > 0$ and $J_1, J_3 < 0$, *i.e.* the relevant parameter region for $\text{Cu}_3\text{Cl}_6(\text{H}_2\text{O})_2 \cdot 2\text{H}_8\text{C}_4\text{SO}_2$. Unfortunately, however, the fields required to polarize this material completely are clearly outside the experimentally accessible range [15].

- [1] K. Hida, J. Phys. Soc. Jpn. **63**, 2359 (1994).
- [2] K. Okamoto, Solid State Communications **98**, 245 (1996).
- [3] D.C. Cabra and M.D. Grynberg, Phys. Rev. **B59**, 119 (1999).
- [4] A. Honecker, Phys. Rev. **B59**, 6790 (1999).
- [5] K. Okamoto and A. Kitazawa, J. Phys. A: Math. Gen. **32**, 4601 (1999).
- [6] B. Sutherland and B.S. Shastry, J. Stat. Phys. **33**, 477 (1983).
- [7] M.W. Long and R. Fehrenbacher, J. Phys.: Condensed Matter **2**, 2787 (1990).
- [8] M.W. Long and S. Siak, J. Phys.: Condensed Matter **2**, 10321 (1990).
- [9] K. Takano, J. Phys. A: Math. Gen. **27**, L269 (1994).
- [10] K. Takano, K. Kubo and H. Sakamoto, J. Phys.: Condensed Matter **8**, 6405 (1996).
- [11] M.R. Bond, R.D. Willett, R.S. Rubins, P. Zhou, C.E. Zaspel, S.L. Hutton and J.E. Drumheller, Phys. Rev. **B42**, 10280 (1990).
- [12] Y. Ajiro, T. Asano, T. Inami, H. Aruga-Katori and T. Goto, J. Phys. Soc. Jpn. **63**, 859 (1994).
- [13] D.D. Swank and R.D. Willett, Inorganica Chimica Acta **8**, 143 (1974).
- [14] D.D. Swank, C.P. Landee and R.D. Willett, Journal of Magnetism and Magnetic Materials **15**, 319 (1980).
- [15] M. Ishii, H. Tanaka, M. Hori, H. Uekusa, Y. Ohashi, K. Tatani, K. Kindo and Y. Narumi, J. Phys. Soc. Jpn. **69**, 340 (2000).
- [16] The low-temperature susceptibility of [15] is substantially lower than that of [14]. The authors of [15] suggested that this discrepancy may be due to a large impurity contribution in [14].
- [17] We use the notations of [18] which differ from [15] by exchanging J_2 and J_3 .
- [18] K. Okamoto, T. Tonegawa, Y. Takahashi and M. Kaburagi, J. Phys.: Condensed Matter **11**, 10485 (1999).
- [19] T. Sano and K. Takano, preprint cond-mat/0005281.
- [20] T. Tonegawa, K. Okamoto, T. Hikihara, Y. Takahashi and M. Kaburagi, preprint cond-mat/9912482.
- [21] <http://www.tu-bs.de/~honecker/trimer/>
<http://www.itp.phys.ethz.ch/staff/laeuchli/trimer>
- [22] The price to pay for using an elementary approach is a substantial amount of CPU time even on modern workstations.

- [23] G.A. Baker Jr., G.S. Rushbrooke and H.E. Gilbert, Physical Review **135**, A1272 (1964); A. Bühler, N. Elstner and G.S. Uhrig, preprint cond-mat/0003221, to appear in Eur. Phys. J. **B**.
- [24] M. Ishii and H. Tanaka, private communication.
- [25] A. Honecker, F. Mila and M. Troyer, Eur. Phys. J. **B15**, 227 (2000).
- [26] S.K. Pati, S. Ramasesha and D. Sen, Phys. Rev. **B55**, 8894 (1997).
- [27] \mathcal{J}_2 changes sign inside the region with $\mathcal{J}_1 > 0$ such that $\mathcal{J}_2 < 0$ throughout the region with $\mathcal{J}_1 < 0$. \mathcal{J}_2 is therefore not relevant to the transition.
- [28] S. Eggert, Phys. Rev. **B54**, R9612 (1996).
- [29] We stopped at fifth order because terms that are not contained in (5.2) would start to appear at the sixth order.
- [30] R. Roth and U. Schollwöck, Phys. Rev. **B58**, 9264 (1998).
- [31] D.C. Cabra, A. Honecker and P. Pujol, Eur. Phys. J. **B13**, 55 (2000).
- [32] K. Totsuka, Phys. Rev. **B57**, 3454 (1998); Eur. Phys. J. **B5**, 705 (1998).
- [33] F. Mila, Eur. Phys. J. **B6**, 201 (1998).
- [34] G. Chaboussant, M.-H. Julien, Y. Fagot-Revurat, M. Hanson, C. Berthier, L.P. Lévy, M. Horvatić and O. Pi-ovesana, Eur. Phys. J. **B6**, 167 (1998).
- [35] K. Tandon, S. Lal, S.K. Pati, S. Ramasesha and D. Sen, Phys. Rev. **B59**, 396 (1999).
- [36] A. Furusaki and S.C. Zhang, Phys. Rev. **B60**, 1175 (1999).
- [37] S. Wessel and S. Haas, preprint cond-mat/9905331; preprint cond-mat/9910259.